AN OVERVIEW OF THE MARS ATMOSPHERIC STATE AS OBSERVED BY EMIRS

Michael D. Smith, *NASA Goddard Space Flight Center, Greenbelt, MD, USA (Michael.D.Smith@nasa.gov),* **K. Badri, E. AlTunaiji,** *Mohammed Bin Rashid Space Center, Dubai, UAE,* **S. A. Atwood**, *LASP, University of Colorado, Boulder, CO, USA.* **C. S. Edwards**, **N. Smith, C. Wolfe**, *Northern Arizona University, Flagstaff, AZ, USA,* **M. J. Wolff**, *Space Science Institute, Boulder, CO, USA,* **P. R. Christensen, S. Anwar**, *Arizona State University, Tempe, AZ, USA.*

Introduction: Thermal infrared spectra taken by The Emirates Mars Infrared Spectrometer (EMIRS) (Edwards et al., 2021) on-board the Emirates Mars Mission (EMM) spacecraft (Amiri et al., 2021) are well suited for the retrieval of surface temperatures, the atmospheric temperature profile from the surface to ~50 km, and the column abundance of dust aerosols, water ice clouds, and water vapor. A constrained linear inversion retrieval routine that includes multiple scattering has been developed and optimized for this purpose. The unique, high-altitude orbit of EMM enables sampling of all local times over a wide range of latitudes and longitudes over a short sub-seasonal timescale of less than two weeks. Here, we present an overview of the retrieval algorithm and first atmospheric science results from observations taken by EMIRS over the first Earth year of EMM Science Phase operations.

EMIRS Data: EMIRS is a thermal infrared spectrometer that observes Mars at wavelengths between ~100 and 1600 cm^{-1} (~100 and 6 μm) at a spectral resolution of 5 or 10 cm^{-1}. From its 55-hour period orbit that varies between 20,000 and 43,000 km altitude, EMIRS raster scans the disk of Mars ~20 times during each orbit to provide a global, synoptic view of Mars that samples all local times, day and night. Over the course of approximately 4 orbits (or 10 days), sufficient observations are taken to provide a broad sampling of all local times at nearly all latitudes and longitudes. Although the typical footprint is relatively large (~100–300 km) this spatial resolution is consistent with modern global circulation models and is sufficient to provide a detailed global view of the current climate state.

Retrieval Overview: We follow the constrained linear inversion algorithm of Conrath et al. (2000) and Smith et al. (2006) to retrieve atmospheric state parameters that best match the observed spectra of Mars from EMIRS. The radiative transfer model includes a discrete ordinates treatment of multiple scattering (e.g., Goody & Yung, 1989; Thomas & Stamnes, 1999) to accurately model dust and water ice cloud aerosols, and it accounts for the absorptions from CO_2 and water vapor gases using the HITRAN database (Gordon et al., 2022) and the correlated-k approximation (Lacis & Oinas, 1991).

Given that the spectral signatures of gases and aerosols are relatively well separated in the spectral range observed by EMIRS, the retrieval is performed sequentially for the atmospheric temperature profile, the column optical depths of dust and water ice aerosol, and the column abundance of water vapor. This sequence can be iterated to obtain a self-consistent solution.

There are a number of assumptions that must be made to perform the retrieval. The surface pressure cannot be reliably retrieved with these data and so is instead taken from the Mars Climate Database (MCD) (Forget et al., 1999; Millour et al., 2018). Aerosol optical properties are taken from the work by Wolff et al. (2006). Perhaps most importantly, we must assume a vertical distribution for the aerosols and water vapor. Dust is assumed to follow a Conrath profile (Conrath, 1975). The Conrath-ν parameter is chosen so that the top of the dust layer varies as a function of season and latitude ranging from 1 (aphelion, high latitudes) to 5 scale heights (perihelion, low latitudes) based on prior observations (e.g., Heavens et al., 2011; Smith et al., 2013). Water ice clouds are placed at the water condensation level, while water vapor is well-mixed up to its condensation level.

In these nadir geometry observations, a thermal contrast between the surface and the atmosphere is required in order to observe the absorption (or emission) features from dust, water ice clouds, and water vapor. This thermal contrast becomes vanishingly small near dawn and dusk, which limits our ability to perform the aerosol and water vapor retrievals at those local times. The uncertainty in retrieved parameters is directly related to this thermal contrast, so we compute an estimate for the uncertainty in each retrieved parameter for every retrieval since this uncertainty varies greatly with season, latitude, and local time.

Results: Figure 1 provides an overview of the retrieval results for EMIRS observations taken between 24 May 2021 (L_s=49°) and 24 February 2022 (L_s=180°). The gap between L_s=100° and 120° was caused by the combination of solar conjunction and the spacecraft entering safe mode. Shown are dust extinction column optical depth (referenced to 1075 cm^{-1}), atmospheric temperature (at 0.5 mbar or ~25 km altitude), water ice cloud extinction column optical depth (referenced to 825 cm^{-1}), and the column abundance of water vapor (pr-μm).

The expected aphelion-season variations and interrelations between the four quantities (e.g., Smith, 2004) are evident in Fig. 1. Dust exhibits its annual minimum optical depth, but there was an early season regional dust storm beginning at Ls=153° (see also Badri et al., 2022 for more details). Atmospheric temperatures become warmer as the season progresses and they respond rapidly to the onset of the regional dust storm. The aphelion season water ice cloud belt dominates the third panel of Figure 1 with additional polar clouds appearing later in the season (see also Atwood et al., 2022 for more details). Finally, the high-latitude northern hemisphere summer maximum and subsequent equatorward transport of water vapor is well documented by the EMIRS retrievals.

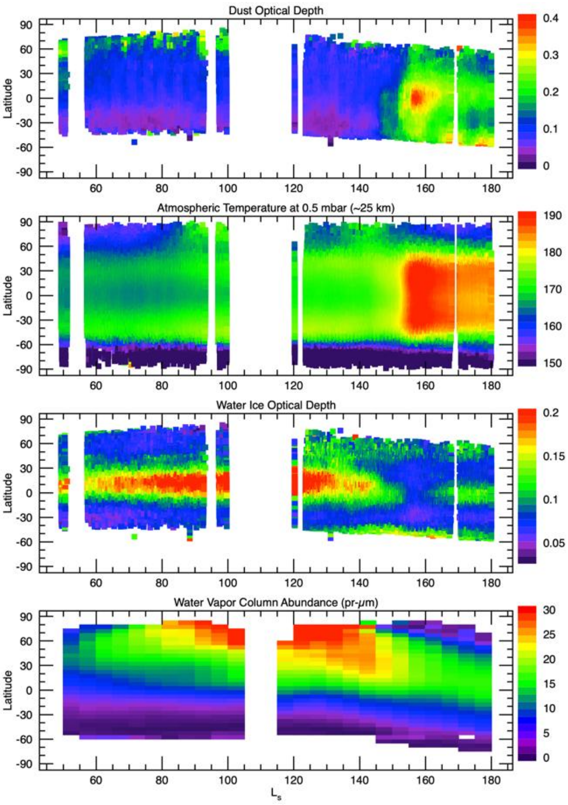

Figure 1: The seasonal and latitudinal variation of **(top)** dust column-integrated optical depth, **(second)** atmospheric temperature at 0.5 mbar (~25 km), **(third)** water ice cloud column-integrated optical depth, and **(bottom)** water vapor column abundance (pr-μm) as retrieved from EMIRS observations.

Figure 2 shows atmospheric temperature cross-sections for two different seasons during Northern-Hemisphere Spring (L_s=55°–70°) and just before Northern Hemisphere Autumn equinox (L_s=160°–175°) retrieved from EMIRS afternoon observations. These retrievals include thermal variations caused by the general circulation, tides, waves, and radiative processes (see also, Fan et al., 2022; Young et al., 2022).

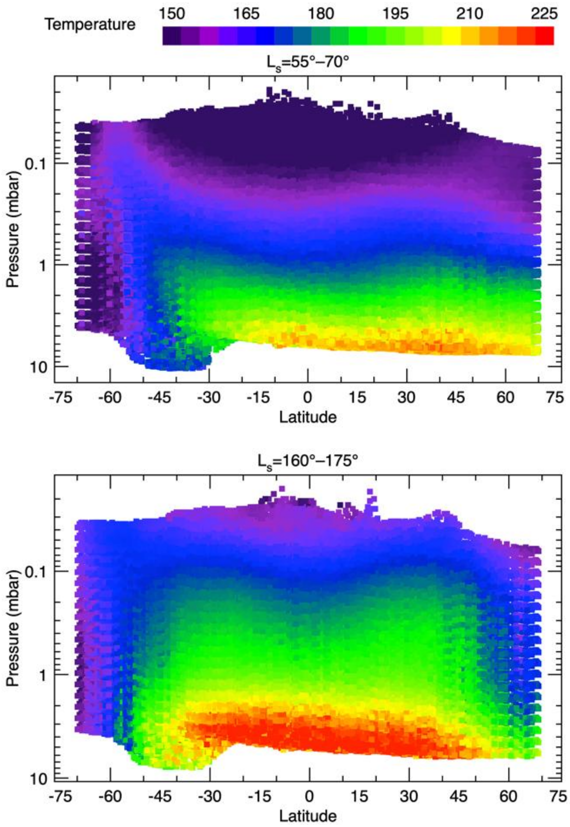

Figure 2: Latitude-pressure cross-sections of atmospheric temperatures retrieved from EMIRS observations for two different seasons.

Summary: The unique orbit of the Emirates Mars Mission enables nearly the entire atmosphere of Mars to be sampled over all local times on timescales as short as 10 days. The thermal infrared spectra observed by the EMIRS instrument are well suited for the retrieval of atmospheric temperature profiles and the column-integrated quantities of dust and water ice aerosol optical depth and of water vapor abundance. The thermal structure and the spatial variations of aerosols and water vapor were as expected for the aphelion season that has so far been observed. Clear diurnal variations in atmospheric temperatures and water ice cloud opacity are evident in the retrievals (see Atwood et al., 2022; Fan et al., 2022 for details). Detailed analysis of these retrieval results will improve our understanding of the underlying physical processes while also helping to validate and tune GCM models. Systematic EMIRS observations continue as the part of the baseline set of ongoing EMM observations promising exciting new information as we enter the dusty perihelion season.

References:

Amiri, H.E. S. et al., 2021. *Space Sci. Reviews*, **218:4**, doi:10.1007/s11214-021-00868-x.

Atwood, S.A., et al., 2022. *The diurnal and seasonal variation of water ice clouds as observed by EMIRS.* 7th Mars Atmosphere Modeling and Observations conference, Paris.

Badri, K., et al., 2022. *The diurnal and seasonal variation of dust aerosol as observed by EMIRS.* 7th Mars Atmosphere Modeling and Observations conference, Paris.

Conrath, B.J., 1975. *Icarus*, **24**, 36–46.

Conrath, B.J. et al, 2000. *J. Geophys. Res.*, **105**, E4, 9509–9519.

Edwards, C.S. et al., 2021. *Space Sci. Reviews*, **217:77**, doi:10.1007/s11214-021-00848-1.

Fan, S. et al., 2022. *Migrating thermal tides in the Martian atmosphere during aphelion season observed by EMM/EMIRS*. 7th Mars Atmosphere Modeling and Observations conference, Paris.

Forget, F. et al., 1999. *J. Geophys. Res.*, **104**, E10, 24155–24176.

Goody, R.M. & Yung, Y.L., 1989. *Atmospheric Radiation: Theoretical Basis*. Oxford Univ. Press.

Gordon, I.E., et al., 2022. *JQSRT*, **277**, doi:10.1016/j.jqsrt.2021.107949.

Heavens, N.G., et al., 2011. *J. Geophys. Res.*, **116**, E04003, doi:10.1029/2010JE003691.

Lacis, A.A. & Oinas, V., 1991. *J. Geophys. Res*., **96**, 9027–9063.

Millour, E. et al., 2018. "From Mars Express to ExoMars" workshop. ESAC Madrid, Spain. https://www.cosmos.esa.int/documents/1499429/1583871/Millour_E.pdf

Smith, M.D., 2004. *Icarus*, **167**, 148–165.

Smith, M.D., et al., 2006. *J. Geophys. Res.*, **111**, E12S13, doi:10.1029/2006JE002770.

Smith, M.D., et al., 2013. *J. Geophys. Res.*, **118,** 1–14, doi:10.1002/jgre.20047.

Thomas, G.E. & Stamnes, K., 1999. *Radiative Transfer in the Atmosphere and Ocean*, Cambridge Univ. Press.

Wolff, M.J., et al., 2006. *J. Geophys. Res.*, **111**, E12S17, doi:10.1029/2006JE002786.

Young, R. et al., 2022. *Atmospheric data assimilation with the Emirates Mars Mission.* 7th Mars Atmosphere Modeling and Observations conference, Paris.